Epimerization of Chlorophyll Derivatives. V. Effects of the Central Magnesium and Ring Substituents on the Epimerization of Chlorophyll Derivatives

Hitoshi Mazaki, Tadashi Watanabe,* Terumi Takahashi,
Andreas Struck,† and Hugo Scheer†
Institute of Industrial Science, The University of Tokyo,
Roppongi, Minato-ku, Tokyo 106
† Botanical Institute, The University of Munich,
D-8000 Munich 19, Germany

(Received June 29, 1992)

Kinetic and equilibrium features of the epimerization in six C13^2-epimer pairs of chlorophyllous pigments, namely chlorophyll (Chl) *a*/*a*′, Chl *b*/*b*′, pheophytin (Pheo) *a*/*a*′, Pheo *b*/*b*′, C20-chlorinated Chl (Cl-Chl) *a*/*a*′, and Cl-Pheo *a*/*a*′, catalyzed by bases (triethylamine, pyrrolidine, and piperidine) and by Lewis acids (magnesium acetylacetonate and magnesium chloride), have been studied in diethyl ether and methanol. A significant difference was noted in the epimerization rate and equilibrium epimeric composition among the pigment systems. The difference in the rate constants was rationalized in terms of the ease in C13^2-proton detachment, affected by the ring π-electron density which in turn depends on the electron donation or withdrawal by the central metal and/or ring substituents. For Lewis acid-catalysis, a dominant factor appears to be the stabilization of the C13^1-enolate anion via formation of a loose complex with extraneous Mg^{2+}. A synergistic action of a base (triethylamine) and a Lewis acid (Mg^{2+}) was observed for the epimerization or enolization of Pheo *a*/*a*′ in methanol.

Chlorophyllous pigments, except for bacteriochlorophyll (BChl) *c*, *d*, and *e* lacking the relevant moieties, are known to undergo epimerization, namely the reversible stereoisomerization at carbon 13^2, and an epimer pair is denoted with a non-primed and primed symbol, e.g., as chlorophyll (Chl) *a*/*a*′ (Fig. 1). Recent discovery of primed pigments as a minor but probably essential component of the higher plant photosystem I reaction center[1] and of heliobacterial reaction centers[2] prompts us to closely study the features of epimerization, in relation to their biosynthetic pathways and stability in vivo. Epimerization is also of primary concern in characterizing the pigments in vitro, since this reaction takes place readily under certain conditions and the epimers, despite a nearly identical visible absorption spectrum in the monomeric state,[3] behave quite differently with respect to molecular polarity, NMR and CD spectrum, and intermolecular association.[4] More importantly, study of the epimerization kinetics would unravel a relationship between the molecular structure and electronic properties of chlorophylls, because the reaction is caused by a nucleophilic and/or electrophilic attack of extraneous species.

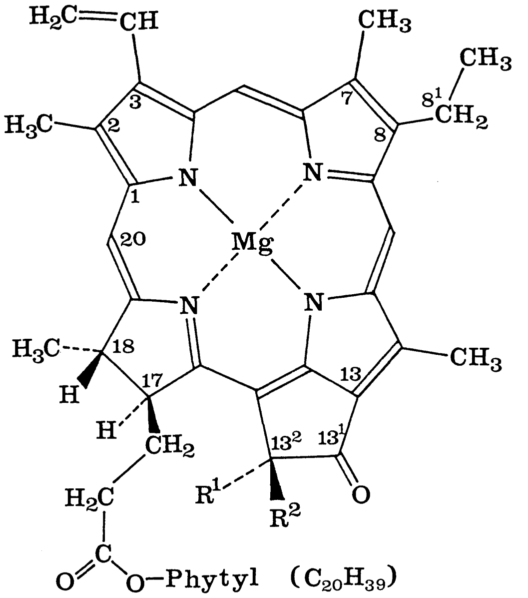

Fig. 1. Structures of Chl *a* (R^1=COOCH$_3$, R^2=H) and Chl *a*′ (R^1=H, R^2=COOCH$_3$) with partial carbon numbering according to the IUPAC system. The Chl *b*/*b*′ pair possesses CHO instead of CH$_3$ at carbon 7. Replacement of the central Mg^{2+} ion with two protons gives pheophytins.

Due mainly to the lack of an analytical tool enabling rapid and reliable assay of the epimeric composition, the number of works on Chl epimerization has been limited.[5–8] In view of this we developed a rapid, high-resolution HPLC technique and applied it to investigations of base-catalysis[9–11] and self-catalysis[12] of two pigment systems, Chl *a*/*a*′ and pheophytin (Pheo) *a*/*a*′. As an extension of these works, we now compare systematically the thermodynamic and kinetic features of Chl *a*/*a*′, Chl *b*/*b*′, Pheo *a*/*a*′, Pheo *b*/*b*′, C20-chlorinated Chl (Cl-Chl) *a*/*a*′, and Cl-Pheo *a*/*a*′ epimerizations catalyzed by bases and Lewis acids, to probe into the effects of the central metal and ring substituents on the electronic state of the molecules. The Lewis acid-catalyzed epimerization is what we found for the Chl *a*/*a*′ and Pheo *a*/*a*′ systems in a foregoing work,[12] and some preliminary data were presented there. The choice of C20-chlorinated pigments in the present work is based on a possibility that Cl-Chl *a* is an intermediate in the metabolic degradation of Chl *a* in vivo,[13] though the once-claimed role of C13^2-hydroxylated Cl–Chl *a* as a component of reaction center I[14] has been disproved later.[15,16] Because of a fairly complicated nature of the reaction, the discussion on the experimental results is limited to a qualitative or semiquantitative level, and a thorough elucidation of the molecular mechanism is beyond the scope of this paper.

Experimental

Chl *a* and *b* were extracted from *Chlorella*. Their pheophytinization and epimerization followed by preparative scale HPLC purification[4] gave Chls and Pheos in *a*, *a'*, *b*, and *b'* forms. C20-chlorinated Chl *a*/*a'* and Pheo *a*/*a'* were prepared according to the procedure described elsewhere.[13,16] Triethylamine, pyrrolidine, and piperidine were used as base catalysts, and magnesium acetylacetonate ($Mg(acac)_2$) and anhydrous $MgCl_2$ were as Lewis acid catalysts. All these chemicals were of reagent grade and used as received. The solvent for epimerization runs was either diethyl ether or methanol (Wako Pure Chemical Ind.). Further purification of the solvents was not performed since, in a preliminary experiment, no difference was noted for the Chl *a*/*a'* epimerization kinetics before and after additional distillation of diethyl ether.

The kinetic and thermodynamic features of epimerization, expressed for the Chl *a*/*a'* system as an example with pseudo-first order rate constants *k* and *k'*,

$$\text{Chl } a \underset{k'}{\overset{k}{\rightleftharpoons}} \text{Chl } a' \tag{1}$$

were analyzed, via HPLC measurements of epimeric composition as a function of time, in terms of the following formulae:[9-12]

$$\frac{[a']_t - [a']_\infty}{[a']_0 - [a']_\infty} = \exp[-(k+k')t] = \exp(-t/\tau) \tag{2}$$

$$[a']_\infty = k/(k+k') \tag{3}$$

$$K = [a']_\infty/[a]_\infty = k/k' \tag{4}$$

$$\Delta G^\circ = -RT \ln K \tag{5}$$

Here $[a']_t$, $[a']_0$, and $[a']_\infty$ denote the mole fraction of the primed species at time *t*, at the onset of measurement, and at equilibrium, respectively, τ the epimerization time constant defined by $(k+k')^{-1}$, *K* the equilibrium constant for reaction (1), and ΔG° the standard Gibbs free energy change by the Chl $a \rightarrow a'$ transformation.

Results and Discussion

Base-Catalyzed Epimerization in Diethyl Ether. As a typical example, Fig. 2 depicts the Chl *b*/*b'* epimerization rate constant ($k+k'$) in diethyl ether at 25 °C against the concentration of three amines. The equilibrium mole fraction of Chl *b'*, $[b']_\infty$, was 0.220 at this temperature. This is the first case, to our knowledge, where the Chl *b*/*b'* epimerization has been studied quantitatively. The rate constant is proportional to the catalyst (base) concentration, and the catalytic activity is higher for a base of larger pK_a value. These features are entirely identical to those of Chl *a*/*a'* epimerization,[11] and indicate that the Chl *b*/*b'* epimerization proceeds via base catalysis: Abstraction of the C13^2-proton by a base gives a transient enolate anion at the β-keto ester system of the cyclopentanone ring, and the enolate anion, upon recombination of the 13^2-carbon with a proton, yields one of the epimers at a probability determined by energetics. The $k+k'$ value for Chl *b*/*b'* is about sevenfold larger than that for Chl *a*/*a'* at a common base concentration.[11]

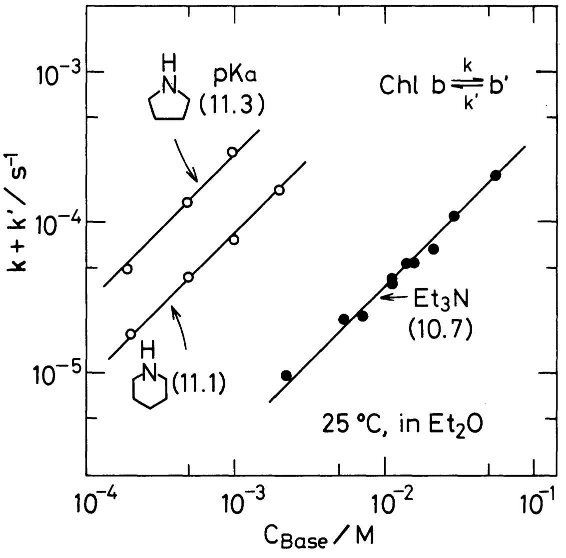

Fig. 2. Dependence of the Chl *b*/*b'* epimerization rate constant ($k+k'$) on the concentration of amines (pyrrolidine, piperidine, and triethylamine) used as catalysts.

A series of measurements have been performed by selecting triethylamine (Et_3N) as the base catalyst. Figure 3 illustrates the results for the four C20-unchlorinated epimer pairs, Chl *a*/*a'*, Chl *b*/*b'*, Pheo *a*/*a'*, and Pheo *b*/*b'*. As is seen, for each pigment system the rate constant exhibits first order dependence on the triethylamine concentration, suggesting that the reaction mechanism is common among them. A similar behavior was observed also for C20-chlorinated pigments. Table 1 summarizes the kinetic and thermodynamic parameters obtained for a total of six pigment systems, together with those of two bacteriochlorophylls (BChls) just for comparison. It is seen that the epimerization rate as well as the equilibrium epimer composition depends heavily on the nature of pigment.

For C20-unchlorinated pigment systems, the order of the $k+k'$ value under identical conditions is

Pheo *b*/*b'* > Pheo *a*/*a'* > Chl *b*/*b'* > Chl *a*/*a'*

with approximate relative ratios of 150 : 40 : 7 : 1. This

Table 1. Kinetic and Thermodynamic Parameters for the Epimerization of Chlorophyll Derivatives at 25 °C in Diethyl Ether Containing 0.01 M Triethylamine

Pigment system	Epimn. rate const $k+k'$	Epimn. time const τ	Equil. mole fraction $[a']_\infty$ or $[b']_\infty$	ΔG° for $a\,(b) \rightarrow a'\,(b')$
	s^{-1}	h	—	kJ mol^{-1}
Pheo *b*/*b*′	8.09×10^{-4}	0.34	0.127	4.78
Pheo *a*/*a*′	2.11×10^{-4}	1.3	0.173	3.88
Cl-Pheo *a*/*a*′	1.82×10^{-4}	1.5	0.182	3.73
Chl *b*/*b*′	3.84×10^{-5}	7.2	0.220	3.14
Cl-Chl *a*/*a*′	8.20×10^{-6}	34	0.235	2.93
Chl *a*/*a*′	5.42×10^{-6}	51	0.240	2.86
BChl *g*/*g*′[a)]	2.14×10^{-6}	130	0.246	2.78
BChl *a*/*a*′[a)]	2.10×10^{-7}	1300	0.250	2.72

a) Unpublished data listed for comparison. BChl *g* and BChl *a* are the major pigments in heliobacteria and purple photosynthetic bacteria, respectively. Since the epimerization rates of these pigments were extremely low, the kinetic experiments were conducted at a triethylamine concentration of 0.1 M, and the measured rate constants were reduced tenfold.

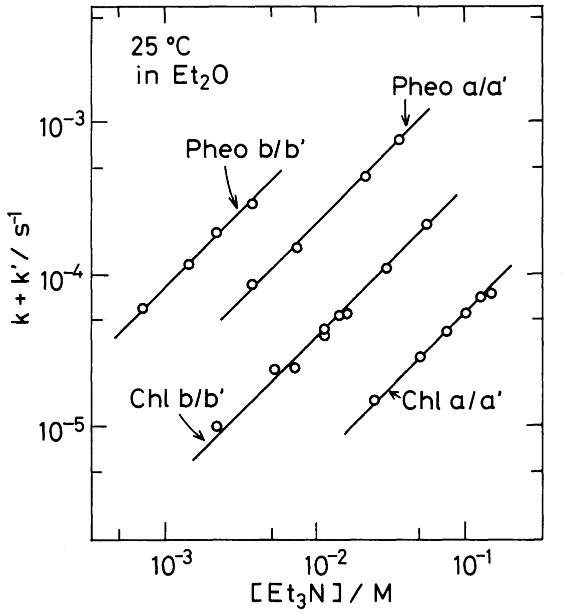

Fig. 3. Dependence of the triethylamine-catalyzed epimerization rate constants on the triethylamine concentration, for the four pigment systems.

order is clearly inverse to that of the ring π-electron density, which is affected by an inductive effect of the central metal (Mg in Chls and H_2 in Pheos) and substituent groups.[17)] Thus, a Pheo species has a lower π-electron density than a Chl species because of a higher electron affinity of the hydrogen atom (Pauling's electronegativity $\chi_P=2.1$) as compared with the Mg atom ($\chi_P=1.2$). Similarly, the π-electron density in a *b*-type pigment is lowered by a higher tendency of electron withdrawal by the C7-CHO group (Hammett's meta-substituent constant $\sigma_m=0.355$) than by the CH_3 group ($\sigma_m=-0.069$) in an *a*-type pigment. This order is well in line with the redox potentials of the pigments.[18)]

The base-catalyzed epimerization proceeds, as mentioned above, via formation of an enol (or enolate anion plus proton) at the cyclopentanone ring, in which the C13^1-carbonyl takes a form of C–O$^-$, C13^2 and C13^1 are connected by a double bond, and the C13^2-proton is transiently detached. In the enol form the cyclopentanone ring is conjugated with the macrocycle π-system, as evidenced by a drastic change in the UV-visible absorption spectrum.[19,20)] When the molecule is in a perfect keto form as in Fig. 1, carbon 13^2 lacks π-electron density as seen from *ab initio* MO calculations on ethyl chlorophyllide *a* and ethyl pheophorbide *a*.[21)] In this case, therefore, the ring π-electron density could not control the epimerization rate. However, Chls in polar organic solvents are known to be in equilibrium between the keto and enol forms, though the fraction of the latter is very small in ordinary media.[20)] The effect of the ring π-electron density on the base-catalyzed epimerization rate could thus be rationalized by invoking such π-conjugation, affecting the C13^2 electron density and hence the ease in C13^2-proton detachment, in the enol form of Chl derivatives.

A steric effect, in addition to the electronic effect mentioned above, also may be a cause for the accelerated epimerization of a Pheo species as compared to a Chl species, since an increased flexibility of the chlorin ring in the former molecule[16)] may facilitate the keto/enol interconversion.

The effect of C20-chlorination is rather small here. Thus, a 50-% increase and a 10-% decrease in the rate constant are noted by C20-chlorination of the Chl *a*/*a*′ and Pheo *a*/*a*′ system, respectively (Table 1). The small effect of the Cl-substituent, despite its high σ_m value (0.373), on the epimerization rate may be due to a back donation of lone pair electrons, which suppresses the inductive effect, and/or to a steric hindrance by the bulky chlorine atom.[13)]

Temperature Dependence of Base-Catalyzed Epimerization in Diethyl Ether. Figure 4 shows, as a function of reciprocal temperature, the equilibrium epimer composition ($[a']_\infty$ and $[b']_\infty$ in percent) for the four pigment systems, and the $-\ln K$ value derived therefrom, in diethyl ether. For reasons of sample availability, the equilibrium epimeric compositions of

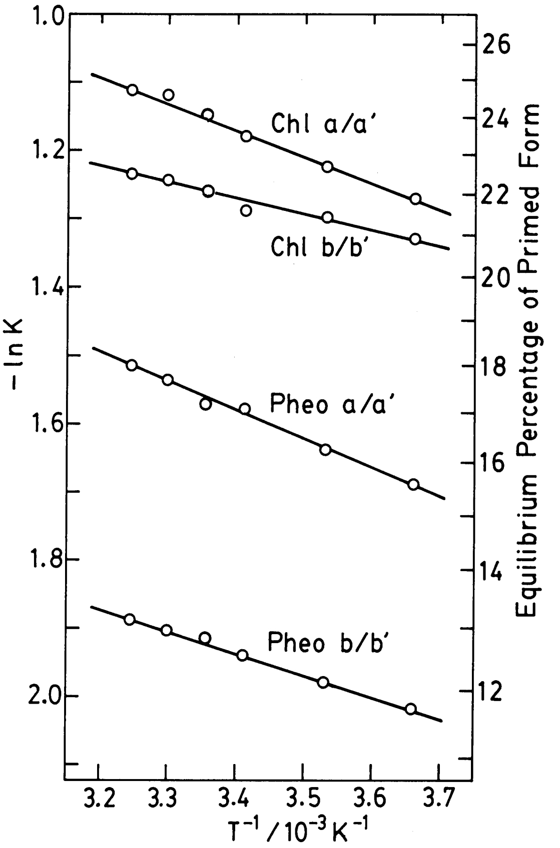

Fig. 4. Temperature dependence of the equilibrium epimeric composition or the equilibrium constant K in diethyl ether for the four pigment systems.

C20-chlorinated species were measured only at 25 °C, and the values for Cl–Chl *a*/*a*′ and Cl–Pheo *a*/*a*′ listed in Table 1 are fairly close to those for the corresponding unchlorinated species.

The standard Gibbs free energy change $\Delta G°$ for the process $a \rightarrow a'$ or $b \rightarrow b'$ is calculated according to Eq. 5. Since $\Delta G°$ is equal to $\Delta H° - T\Delta S°$, where $H°$ denotes the standard enthalpy and $S°$ the standard entropy, the $\Delta H°$ values were calculated from the slope of a line in Fig. 3 to obtain 3.2, 2.0, 3.6, and 2.6 kJ mol^{-1} for the Chl *a*/*a*′, Chl *b*/*b*′, Pheo *a*/*a*′, and Pheo *b*/*b*′ systems, respectively. In a separate series of experiments we measured the rate constant $k+k'$ as a function of temperature, and the forward (k) and backward (k') rate constants were calculated by combining the kinetic data with the equilibrium data (Fig. 4) based on Eq. 3. Activation energies thus determined are given in Table 2. The difference in the activation energy between the forward and backward reaction nicely agrees with the $\Delta H°$ value obtained above. The rate constant at a given temperature in a range from 0 to 34 °C can be obtained by combining Tables 1 and 2.

Table 2. Activation Energies for the Triethylamine-Catalyzed Epimerization in Diethyl Ether[a)]

Pigment system	Activation energy E_a/kJ mol^{-1}		ΔE_a
	Forward (k)	Backward (k')	kJ mol^{-1}
Chl *a*/*a*′	43.6	40.2	3.4
Chl *b*/*b*′	45.1	43.2	1.9
Pheo *a*/*a*′	43.4	39.6	3.8
Pheo *b*/*b*′	39.5	36.8	2.7

a) Temperature range for measurement, 0—34 °C.

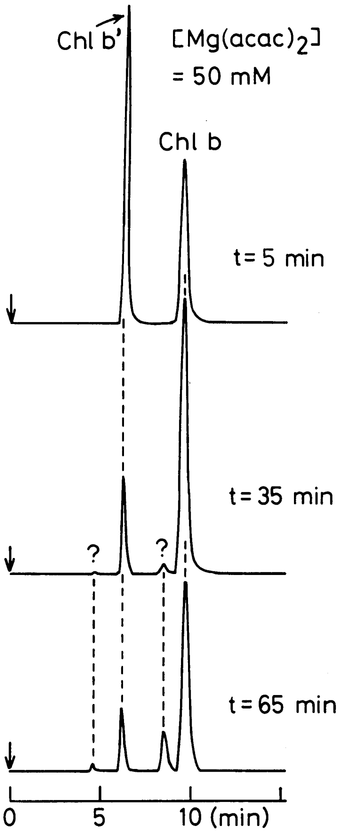

Fig. 5. Temporal evolution of HPLC traces for Chl *b*′ in the presence of 50 mM Mg(acac)$_2$ in methanol. Question marks denote unidentified side products. Column, 5-μm silica (150×4.6 mm i.d.); eluent, hexane/2-propanol (100/1.5, v/v); flow rate, 1.5 ml min^{-1}; detection wavelength, 450 nm.

Mg(acac)$_2$-Catalyzed Epimerization in Methanol. Chl *a*/*a*′ and Pheo *a*/*a*′ underwent epimerization in the presence of Mg(acac)$_2$ instead of an amine, and this phenomenon was interpreted[12)] as due to a Lewis acid-catalysis, where an electrophilic attack of the Mg compound at the β-keto ester system of the cyclopentanone ring is followed by dissociation/recombination of the C13^2-proton.

The rate constants of this process have been measured for the six pigment systems in methanol, which was employed for reasons of Mg(acac)$_2$ solubility. In contrast to the pigments in neat methanol, where a rapid allomerization (oxidative degradation of the cyclopentanone ring) takes place,[22,23)] epimerization was almost the sole process in the presence of Mg(acac)$_2$. For the Chl

Table 3. Kinetic and Thermodynamic Parameters for the Epimerization of Chlorophyll Derivatives at 25 °C in Methanol Containing 0.01 M Magnesium Acetylacetonate

Pigment system	Epimn. rate const $k+k'$	Epimn. time const τ	Equil. mole fraction $[a']_\infty$ or $[b']_\infty$	$\Delta G°$ for $a\,(b) \rightarrow a'\,(b')$
	s^{-1}	min	—	kJ mol^{-1}
Pheo *b*/*b′*[a]	1.67×10^{-2}	1.0	0.10	5.4
Cl-Pheo *a*/*a′*[a]	4.98×10^{-3}	3.4	0.16	4.1
Pheo *a*/*a′*	2.07×10^{-3}	8.1	0.13	4.7
Chl *b*/*b′*	3.74×10^{-4}	45	0.16	4.1
Cl-Chl *a*/*a′*	2.67×10^{-4}	62	0.21	3.3
Chl *a*/*a′*	1.91×10^{-4}	87	0.17	3.9

a) Rate constants were obtained by extrapolation of the data acquired in a $Mg(acac)_2$ concentration range of 10^{-4}—2×10^{-3} M.

b/*b′* system alone, some additional reaction accompanied epimerization as noted for the HPLC traces shown in Fig. 5. Though these by-products have not been identified, they did not significantly interfere with the determination of the Chl *b*/*b′* epimerization rate constant in the early stage of transformation. As in base catalysis, the epimerization rate constants $k+k'$ were proportional to the $Mg(acac)_2$ concentration in a wide range of the latter, and the results obtained for the six pigment systems, both kinetic and equilibrium data, are summarized in Table 3.

For the C20-unchlorinated pigments, the order of rate constants is

Pheo *b*/*b′* > Pheo *a*/*a′* > Chl *b*/*b′* > Chl *a*/*a′*

with approximate relative ratios of 87 : 11 : 2 : 1. This is qualitatively well in line with that for the base catalysis described above. Also, the order of the equilibrium epimer composition, represented by $[a']_\infty$ or $[b']_\infty$, is apparently common between the two catalyses. These findings strongly suggest that the mode of epimerization is governed by a common factor, namely the ease in $C13^2$-proton detachment, in both base- and Lewis acid-catalysis. Tentatively we envisage the following picture for the Lewis acid-catalysis. A lower π-electron density in the macrocycle tends to detach the $C13^2$-proton as discussed above, thereby yielding a $C13^1$-enolate anion, which is then stabilized by the formation of a loose complex with the Mg atom carrying a partially positive charge in $Mg(acac)_2$. A similar scheme has been established as an initiation step for metal ion-assisted allomerization of Chl.[24]

Upon C20-chlorination, both Chl *a*/*a′* and Pheo *a*/*a′* became more susceptible to $Mg(acac)_2$-catalyzed epimerization by a factor of 1.4 and 2.4, respectively. This is partially in contrast to base-catalyzed epimerization (Table 1) where Cl-Pheo *a*/*a′* exhibits slower epimerization than Pheo *a*/*a′*.

Comparison of Triethylamine- and $Mg(acac)_2$-Catalysis. As described above, the order of kinetic and thermodynamic parameters is very similar between triethylamine- and $Mg(acac)_2$-catalyzed epimerizations for the six pigment systems. However, a subtle difference appears to exist between the two catalyses, probably reflecting a control of the reaction rate by the local electron density in the molecule. In what follows, a pigment system is expressed in the form of "central metal–substituent(s) at C7 (and C20 for chlorinated species)" for convenience. Thus, H_2–CH_3·Cl denotes the Cl–Pheo *a*/*a′* system, though hydrogen is actually not a metal. In triethylamine-catalysis, the ratios of the epimerization rate constant $(k+k')$ under given conditions (Table 1) are as follows:

H_2–CHO : H_2–CH_3·Cl : H_2–CH_3 = 3.8 : 0.86 : 1

Mg–CHO : Mg–CH_3·Cl : Mg–CH_3 = 7.1 : 1.5 : 1

H_2–CHO : Mg–CHO = 21

H_2–CH_3·Cl : Mg–CH_3·Cl = 22

H_2–CH_3 : Mg–CH_3 = 39

Inspection of these figures indicates that the effect of the substituent is more pronounced in Chl (Mg–) species than in Pheo (H_2–) species, and the effect of the central metal is more dominant the more the substituent is electron-donating. These may be rationalized as follows. A Chl species, which has generally a higher ring π-electron density, is unfavorable for the base-catalysis initiated by the nucleophilic attack of a basic compound against the $C13^2$-proton, and hence the effect of the electron-withdrawing substituent (CHO or Cl) is dominant. Similarly, the effect of the central metal is conspicuous when the C7 substituent has a low electron-attracting property (CH_3). In contrast, the ratios of the epimerization rate constant for $Mg(acac)_2$-catalysis (Table 2) are as follows:

H_2–CHO : H_2–CH_3·Cl : H_2–CH_3 = 8.1 : 2.4 : 1

Mg–CHO : Mg–CH_3·Cl : Mg–CH_3 = 2.0 : 1.4 : 1

H_2–CHO : Mg–CHO = 45

H_2–CH_3·Cl : Mg–CH_3·Cl = 19

H_2–CH_3 : Mg–CH_3 = 11

The trend here is neatly opposite to the base-catalysis: the effect of substituents is more pronounced in Pheos than in Chls, and the effect of the central metal is more dominant the more the substituent is electron-withdrawing. This may well reflect the electrophilic attack of Mg(acac)$_2$ against the C13^1-enolate anion. A molecular-level elucidation of these phenomena, however, is not possible at the present stage.

Mg^{2+}-Catalyzed Epimerization. The catalytic effect of Mg^{2+} (from MgCl$_2$) on the epimerization of Chl derivatives was also studied in methanol. Since the presence of Mg^{2+}, in contrast to Mg(acac)$_2$ employed above, resulted in rapid allomerization of the Chl *a*/*a'*, Chl *b*/*b'*, and Cl-Chl *a*/*a'* systems in line with an old report,[24] the data were collected only for Pheo species. The rate constants are very similar among the three pigment systems (Fig. 6), despite the fact that the Pheo *a*/*a'* system underwent epimerization by a factor of 4 to 8 slower than the Pheo *b*/*b'* system in base-catalysis and Mg(acac)$_2$-catalysis, as verified above.

This result may be accounted for as follows. As found in previous work,[12] coexistence of Mg^{2+} and Pheo *a* leads to the formation of a Mg^{2+}–Pheo *a* enolate complex,[20,25] which is stable enough to be observed by visible spectroscopy and is most probably an intermediate in the course of Mg^{2+}-catalysis, whereas in the Mg(acac)$_2$-catalysis such a complex was not observed in the visible spectrum, suggesting that acetylacetone is a much better ligand for Mg^{2+} than the C13^1-carbonyl oxygen of Pheo *a*. In the Mg^{2+} complex, a fairly strong ionic interaction between Mg^{2+} and an enolate anion presumably exists and stabilizes the negative charge on the enolate anion, and this effect should be dominant for an enolate anion with a higher π-electron density in the chlorin ring. For this reason the intrinsic lower stability of the Pheo *a* (*a'*) enolate may not be reflected in the epimerization rate at least.

The Mg^{2+} complex is more stable for Pheo *b* than for Pheo *a* (vide infra), in line with the results thus far, and therefore an easier epimerization of the Pheo *b*/*b'* system due to an intrinsic higher stability of its enolate may be canceled by its slower dissociation in the apparent reaction rate. This may be related to the 5 to 40-fold faster Mg(acac)$_2$-catalysis than the Mg^{2+}-catalysis at a common Mg concentration (Table 3 and Fig. 6).

Synergistic Action of Triethylamine and Lewis Acid in the Epimerization and Enolization of Pheo *a*/*a'*. Epimerization kinetics were investigated in methanolic solutions containing both triethylamine and a Lewis acid, mostly on the Pheo *a*/*a'* system. Figure 7 shows the Pheo *a*/*a'* epimerization rate constant $k+k'$ in the presence and absence of triethylamine (base-catalyst) as a function of [Mg^{2+}]. Triethylamine was used at a single concentration of 0.125 mM, and the $k+k'$ value by this base-catalysis alone was 4.4×10^{-5} s^{-1} (broken line). As seen, by the coexistence of this rather weak catalyst, the rate of Mg^{2+}-catalysis became by two orders-of-magnitude higher than that in its absence. This indicates that Mg^{2+} and triethylamine act cooperatively or synergistically in the epimerization. The synergistic

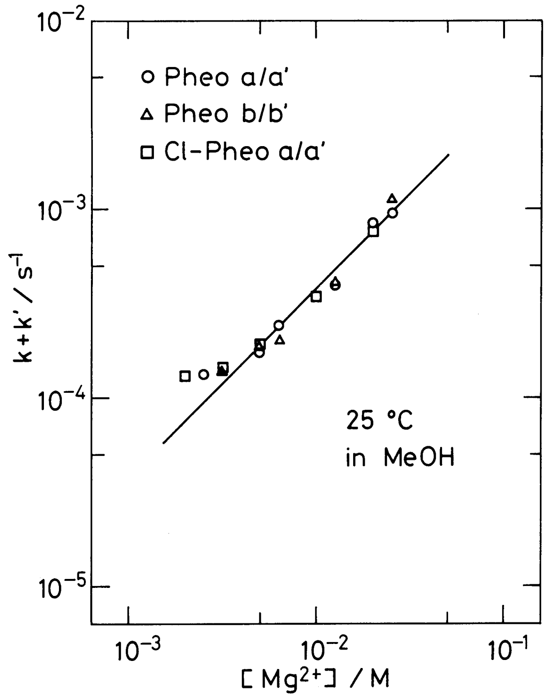

Fig. 6. Dependence of the Pheo *a*/*a'*, Pheo *b*/*b'*, and Cl–Pheo *a*/*a'* epimerization rate constants on the Mg^{2+} concentration in methanol.

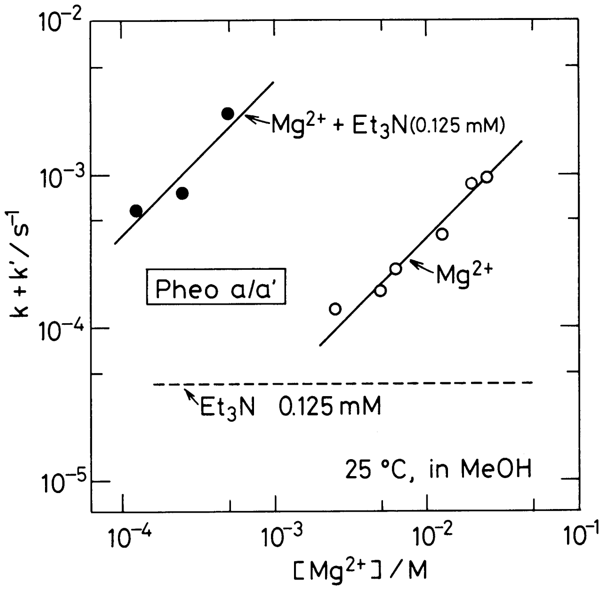

Fig. 7. Dependence of the Pheo *a*/*a'* epimerization rate constant on the Mg^{2+} concentration in the presence or absence of 0.125 mM triethylamine in methanol. Broken horizontal line represents the rate constant by the presence of 0.125 mM triethylamine alone.

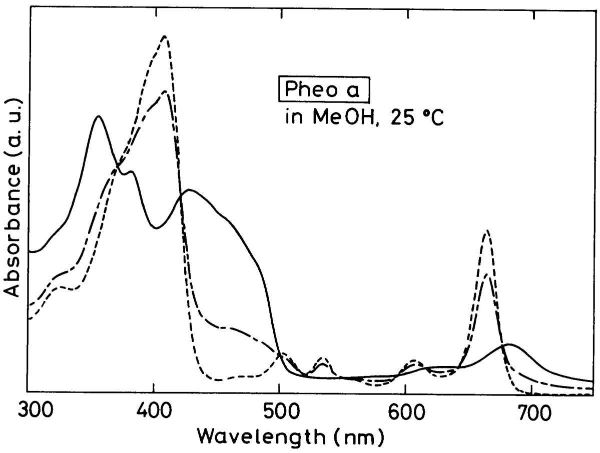

Fig. 8. Absorption spectra of Pheo *a* in methanol: in neat methanol (-----), immediately after addition of 67 mM Mg^{2+} (–•–•–), and by simultaneous addition of 67 mM Mg^{2+} plus 33 mM triethylamine (——).

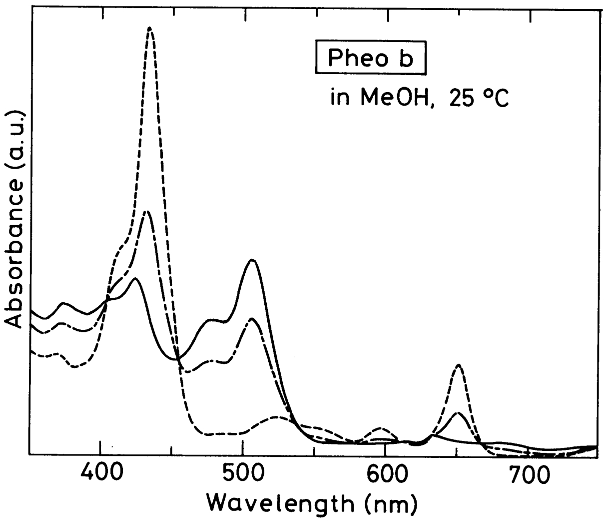

Fig. 9. Absorption spectra of Pheo *b* in methanol. The three curves have the same meanings as in Fig. 8.

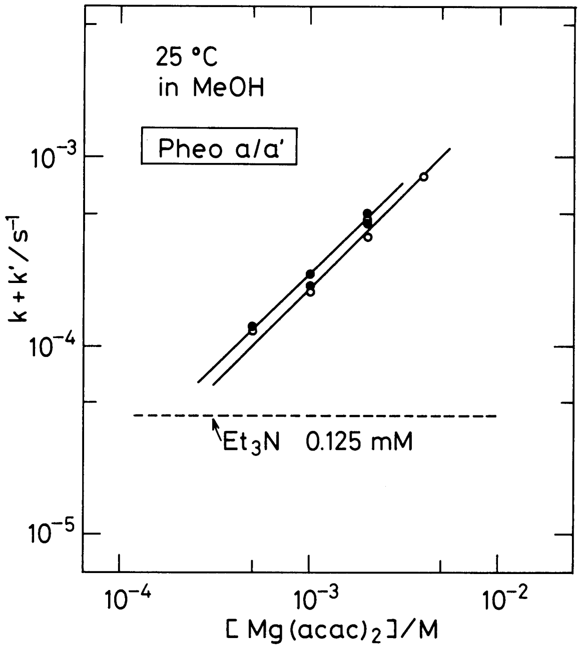

Fig. 10. Dependence of the Pheo *a*/*a*′ epimerization rate constant on the $Mg(acac)_2$ concentration in the presence (●) and absence (○) of 0.125 mM triethylamine in methanol. Broken line represents the rate constant by the presence of 0.125 mM triethylamine alone.

mechanism may consist of almost simultaneous actions of Mg^{2+} and triethylamine onto the $C13^1$-carbonyl oxygen and the $C13^2$-proton, respectively.

Formation of a Mg^{2+}-Pheo *a* enolate complex (enolization), observed at high Mg^{2+} concentrations, is also promoted by the addition of triethylamine (Fig. 8). When the additive was 67 mM Mg^{2+} alone, the fraction of the complex was as small as about 30% immediately after the addition, and was then gradually degraded to the spectrum of intact Pheo *a*. Further addition of 33 mM triethylamine to this solution, however, gave a spectrum essentially identical to that reported by Scheer and Katz[25] as a peripheral Mg^{2+} complex of methyl pheophorbide *a* enolate, and the spectrum remained unchanged for at least 1 h. When only triethylamine was present, even when it was used as solvent, the Pheo *a* enolate anion was not observed at all in the absorption spectrum. Thus, at the stage of enolization, Mg^{2+} should play a role of a main catalyst, triethylamine being a secondary catalyst which supports the action of Mg^{2+}. This is probably the case for the synergistic epimerization described above (Fig. 7). Under identical conditions, Pheo *b* also formed a peripheral complex (Fig. 9) in a manner similar to Pheo *a*, but as much as 65% of the pigment was in the enol form on addition of 67 mM Mg^{2+} alone: This is indeed an indication of a higher stability of Pheo *b* enolate as compared to Pheo *a*.

In contrast, $Mg(acac)_2$ and triethylamine coexisting in methanol apparently did not exhibit a synergistic effect on the Pheo *a*/*a*′ epimerization, as depicted in Fig. 10. A slight increase in the $Mg(acac)_2$-catalyzed epimerization rate constant $k+k'$ by addition of triethylamine is almost at a level of $k+k'$ attained by triethylamine-catalysis alone, suggesting that $Mg(acac)_2$ and triethylamine act independently. This may be due to a fairly large size of the $Mg(acac)_2$ molecule which could suppress a simultaneous attack of triethylamine.

In methanol, a generally observed transformation of Chl derivatives is allomerization.[22,23] When Chl *a* was dissolved in methanol containing Mg^{2+}, a fairly rapid allomerization was indeed observed as reported by Johnston and Watson,[24] and this reaction was accelerated by addition of triethylamine (unpublished results) in a manner similar to the Pheo *a*/*a*′ epimerization shown in Fig. 7. This suggests that allomerization and epimerization occur through a common process of enol formation as proposed previously.[23,26,27] In contrast, when $Mg(acac)_2$ or triethylamine alone was added to a Chl *a* methanolic solution, no allomerization was observed. Despite the catalytic actions of triethylamine and $Mg(acac)_2$ in epimerization, they rather seem to inhibit the allomerization which takes place even in the absence of any catalytic compounds in methanol.[22,23] This particular problem is, however, beyond the scope of the present communication.

References

1) H. Maeda, T. Watanabe, M. Kobayashi, and I. Ikegami, *Biochim. Biophys. Acta,* **1099**, 74 (1992).

2) M. Kobayashi, E. J. van de Meent, C. Erkelens, J. Amesz, I. Ikegami, and T. Watanabe, *Biochim. Biophys. Acta,* **1057**, 89 (1991).

3) T. Watanabe, A. Hongu, K. Honda, M. Nakazato, M. Konno, and S. Saitoh, *Anal. Chem.*, **56**, 251 (1984).

4) T. Watanabe, M. Kobayashi, A. Hongu, and T. Oba, *Chem. Lett.*, **1992**, 1847.

5) J. J. Katz, G. D. Norman, W. A. Svec, and H. H. Strain, *J. Am. Chem. Soc.*, **90**, 6841 (1968).

6) P. H. Hynninen, M. R. Wasielewski, and J. J. Katz, *Acta Chem. Scand., Ser. B,* **33**, 637 (1979).

7) S. Lötjönen and P. H. Hynninen, *Org. Magn. Reson.*, **21**, 757 (1983).

8) P. H. Hynninen and S. Lötjönen, *Org. Magn. Reson.*, **23**, 605 (1985).

9) T. Watanabe, M. Nakazato, M. Konno, S. Saitoh, and K. Honda, *Chem. Lett.*, **1984**, 1411.

10) T. Watanabe, M. Nakazato, and K. Honda, *Chem. Lett.*, **1986**, 253.

11) T. Watanabe, H. Mazaki, and M. Nakazato, *Biochim. Biophys. Acta,* **892**, 197 (1987).

12) H. Mazaki and T. Watanabe, *Biochim. Biophys. Acta,* **1016**, 190 (1990).

13) A. Struck, E. Cmiel, S. Schneider, and H. Scheer, *Photochem. Photobiol.*, **51**, 217 (1990).

14) D. Dörnemann and H. Senger, *FEBS Lett.*, **126**, 323 (1981); *Photochem. Photobiol.*, **35**, 821 (1982); *ibid.*, **43**, 573 (1986).

15) M. Senge, D. Dörnemann, and H. Senger, *FEBS Lett.*, **234**, 215 (1988).

16) M. Kobayashi, T. Watanabe, A. Struck, and H. Scheer, *FEBS Lett.*, **235**, 293 (1988).

17) A. Stanienda, *Z. Phys. Chem.*, **239**, 257 (1965).

18) T. Watanabe and M. Kobayashi, "Chlorophylls," ed by H. Scheer, CRC Press, Boca Raton (1991), pp. 287—315.

19) G. R. Seely, "The Chlorophylls," ed by L. P. Vernon and G. R. Seely, Academic Press, New York (1966), pp. 67—109.

20) P. H. Hynninen, "Chlorophylls," ed by H. Scheer, CRC Press, Boca Raton (1991), pp. 145—209.

21) D. Spangler, G. M. Maggiora, L. L. Shipman, and R. E. Christoffersen, *J. Am. Chem. Soc.*, **99**, 7470, 7478 (1977).

22) P. M. Schaber, J. E. Hunt, R. Fries, and J. J. Katz, *J. Chromatogr.*, **316**, 25 (1984).

23) P. H. Hynninen, *Z. Naturforsch., B,* **36**, 1010 (1981).

24) L. G. Johnston and W. F. Watson, *J. Chem. Soc.*, **1956**, 1203.

25) H. Scheer and J. J. Katz, *J. Am. Chem. Soc.*, **97**, 3273 (1975); *ibid.*, **100**, 561 (1978).

26) P. H. Hynninen, *J. Chromatogr.*, **175**, 75 (1979).

27) A. S. Holt, *Can. J. Biochem. Physiol.*, **36**, 439 (1958).